SQMS Summer Internship Report

Nanofabrication techniques of Josephson junction for transmon qubit

Author : Tommaso Bonaccorsi[*]

Supervisors : Mustafa Bal[†], Francesco Crisa [†]

October 2022

[1]University of Pisa, Department of Physics "E. Fermi"
[2]Superconducting Quantum Materials and Systems Center, Fermi National Accelerator Laboratory

CONTENTS

Abstract

This report deals with the theory of transmon qubits in general, also focusing on the SQUID and the functioning of a Josephson junction. The interaction of the qubit in a cavity with the quantized electro-magnetic field is then treated. After this introduction whose goal is to contextualize the work that I actually did, I will talk about the 2D qubits that we have built. The problem of etching and "patching" will be dealt with in detail, reporting the results obtained in the laboratory. Finally, I wanted to conclude by addressing the concept of measurement of a qubit in a cavity only at a theoretical level. I conclude everything with a "Feynman treatment" of the cavities which in my opinion is really very interesting.

1 TRANSMON QUBIT; *[1] [2] [3] [4]*

1.1 JOSEPHSON JUNCTION THEORY

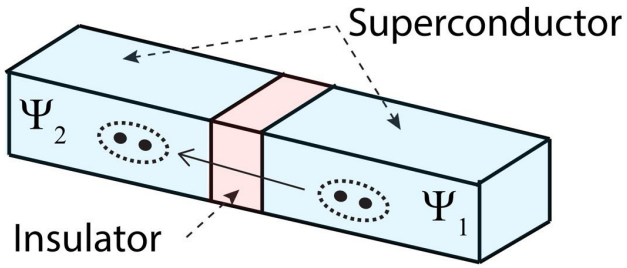

Figure 1: *Structure of Josephson junction (JJ)*

Josephson junction is the case of *superconductor-insulator-superconductor*, besides the quasiparticle tunneling current, we can have also a supercurrent tunneling due to the Cooper pairs transfer between the two superconductors. This current, called Josephson current, can be observed in SIS junctions with extremely thin insulating layers (10-15 Å).
In this situation, the coupling between the two superconductors is sufficiently strong that a definite phase relationship between pairs on opposite sides of the insulating barrier can be maintained.
In particular the direct supercurrent of pairs , for currents less than a certain value I_j, flows with zero voltage drop across the junction (dc Josephson junction).
Consider two superconductors (of the same or different materials) separated by a thin insulating barrier of width b as in the figure below.[1]

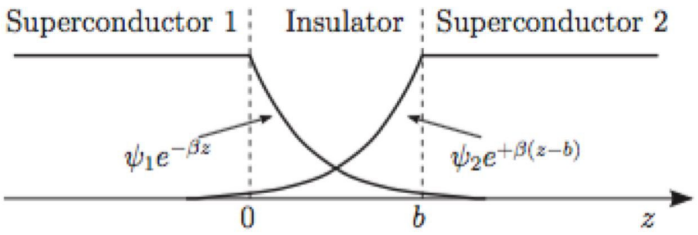

Figure 2: *1D representation of a Josephson junction with the trend of the wave function*

[1] It's very important to note that for this discussion we'll use the Ginzburg-Landau theory, since this theory is very useful for the treatment of the inhomogeneities

If the insulating barrier is infinitely thick we can guess that the order parameter $\psi(z)$ within the barrier can be expressed in the form

$$\psi(z) = \psi_1 e^{-\beta z} + \psi_2 e^{\beta(z-b)} \; 0 < z < b \tag{1}$$

With $\psi_i = |\psi_i| e^{-i\theta_i}$ and the parameter β characterizes the damping within the barrier.
The Schrodinger equation of the system is the following

$$i\hbar \frac{d}{dt} \begin{bmatrix} \psi_1 \\ \psi_2 \end{bmatrix} = \begin{bmatrix} \frac{q_c V}{2} & K \\ K & -\frac{q_c V}{2} \end{bmatrix} \begin{bmatrix} \psi_1 \\ \psi_2 \end{bmatrix} \tag{2}$$

where the parameter K characterizes the tunneling between the barriers, and q_c is the charge of the Cooper pair.
Solving this equation leads to the following results

$$\begin{aligned} I &= I_0 \sin\gamma \\ \frac{d\gamma}{dt} &= \frac{2eV}{\hbar} = \frac{2\pi V}{\Phi_0} \end{aligned} \tag{3}$$

where I_0 depends on the geometrical and physical properties of the junction and $\gamma = \theta_1 - \theta_2$ (phase difference across the junction).
One can then infer that the effective inductance of the Josephson junction is :

$$\begin{aligned} V = L\frac{dI}{dt} \rightarrow \frac{\Phi_0}{2\pi}\frac{d\gamma}{dt} &= L I_0 \frac{d\gamma}{dt}\cos(\gamma) \\ L = \frac{\Phi_0}{2\pi I_0 \cos(\gamma)} \rightarrow L &= \frac{L_{J_0}}{\cos(\gamma)} \end{aligned} \tag{4}$$

where Φ_0 is the flux quantum and we define L_{J_0} as the Josephson junction inductance at zero current. It can be shown that the Josephson junction inductance is a function of the current:

$$\begin{aligned} I = I_0 \sin\gamma \rightarrow (\frac{I}{I_0})^2 &= \sin^2\gamma \\ (\frac{I}{I_0})^2 &= 1 - \cos^2\gamma \end{aligned} \tag{5}$$

Therefore

$$L = \frac{L_{J_0}}{\sqrt{1 - (\frac{I}{I_0})^2}} \tag{6}$$

1.2 **SQUID**

One can use two JJs (assumed to be identical) in a loop to get a tunable JJ where the critical current can be tuned by passing an external flux Φ_{ext} through the loop. Consider a superconducting circuit with two Josephson junctions in parallel.

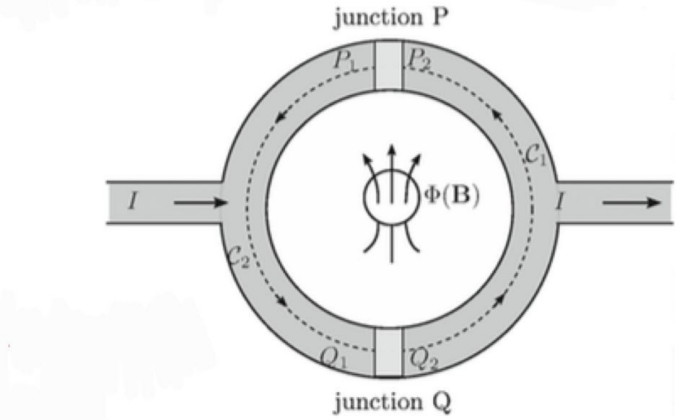

Figure 3: *Illustration of a circuit forming a SQUID. $\mathscr{C}_1$ and $\mathscr{C}_2$ are two circuits inside the ring*

For simplicity we assume that both junctions have the same critical current I_0, that the magnetic flux through the junctions is negligible, and the thickness of the superconducting samples is much larger than the magnetic penetration depth.
The phase differences across the junctions P and Q are $\gamma_p = \theta(P_2) - \theta(P_1)$ and $\gamma_q = \theta(Q_2) - \theta(Q_1)$.
The total current flowing in the circuit is

$$\begin{aligned} I &= I_0(\sin(\gamma_p) - \sin(\gamma_q)) \\ &= 2I_0 \sin(\frac{\gamma_p + \gamma_q}{2}) \cos(\frac{\gamma_p - \gamma_q}{2}) \end{aligned} \tag{7}$$

Inside of the superconductors $J_s = 0$ thus in the Ginzburg-Landau(GL) equation, that we remember to be: :

$$J_s(r) = |\psi(r)|^2 [\frac{e^* \hbar}{m^*} \nabla\theta(r) - \frac{e^{*2}}{m^* c} A(r)] \tag{8}$$

we can put $J_s = 0$ and we get

$$\nabla\theta(r) = -\frac{2e}{\hbar c} A(r) \tag{9}$$

Now we calculate the integrals along $\mathscr{C}_1$ and $\mathscr{C}_2$

$$\begin{aligned} \mathscr{C}_1 &\Longrightarrow \theta(P_2) - \theta(P_1) = -\frac{2e}{\hbar c} \int_{Q_2}^{P_2} \vec{A}(\vec{r}) \cdot d\vec{l} \\ \mathscr{C}_2 &\Longrightarrow \theta(Q_2) - \theta(Q_1) = -\frac{2e}{\hbar c} \int_{P_1}^{Q_1} \vec{A}(\vec{r}) \cdot d\vec{l} \end{aligned} \tag{10}$$

Summing up the two contributions

$$\theta(P_2) - \theta(Q_2) + \theta(Q_1) - \theta(P_1) = -\frac{2e}{\hbar c} \oint \vec{A}(\vec{r}) \cdot d\vec{l} \tag{11}$$

therefore we find

$$\gamma_p - \gamma_q = -\frac{2e}{\hbar c}\Phi(\vec{B}) = -2\pi\frac{\Phi(\vec{B})}{\Phi_0} \tag{12}$$

Inserting this equation in (7), we obtain :

$$I = 2I_0\cos(\pi\frac{\Phi(\vec{B})}{\Phi_0})\sin(\frac{\gamma_p+\gamma_q}{2}) \tag{13}$$

This expression has its maximum value when

$$\sin(\frac{\gamma_p+\gamma_q}{2}) = 1 \tag{14}$$

so ,

$$I_{max} = 2I_0\left|\cos(\pi\frac{\Phi(\vec{B})}{\Phi_0})\right| \tag{15}$$

Since the maximum supercurrent is a periodic function of $\Phi(\vec{B})$ and fluctuates between maxima and minima for flux variations as tiny as $\frac{\Phi_0}{2}$, extremely small magnetic fields can be precisely measured.
The critical value $I_{max}(\Phi)$ denotes the greatest amount of current that can pass through the device without dissipating and with a zero potential voltage across the SQUID.
Let's now examine the overall energy held in a JJ (naturally, a JJ also has some small capacitance, but for our purposes and simplicity we ignore this since we are eventually going to shunt the JJ to a much larger capacitor to make a transmon qubit). The fact that

$$\begin{aligned}
\frac{dU}{dt} &= VI \\
U &= \int_{-\infty}^{t} I(t')V\,dt' \\
&= \frac{I_0\Phi_0}{2\pi}\int_{-\infty}^{t}\sin(\delta)\frac{d\delta}{dt}dt' \\
&= \frac{I_0\Phi_0}{2\pi}[1-\cos(\delta)] \\
&\equiv E_J[1-\cos(\delta)]
\end{aligned} \tag{16}$$

we have assumed that there was no current at t = $-\infty$.

1.3 How to transform an LC circuit into an anharmonic oscillator

To be able to build a qubit we must be able to build a system whose energy levels are quantized but with energies of levels that are not all equal.
In fact, if it were enough to simply have a system with equal discretized energies, it would be enough to take a superconducting LC circuit with very low T (temperature) so that only the lowest levels can be considered populated. Considering the two lower energy levels as qubit.
However, this is not possible.
The energy levels of an LC circuit in quantum regime are all equally spaced, so we cannot work individually on the various levels.
The goal then is to introduce some anharmonicity in this circuit which, however, does not generate dissipation.
Here is the importance of the JJ, it works as a non-linear inductance without adding dissipation.

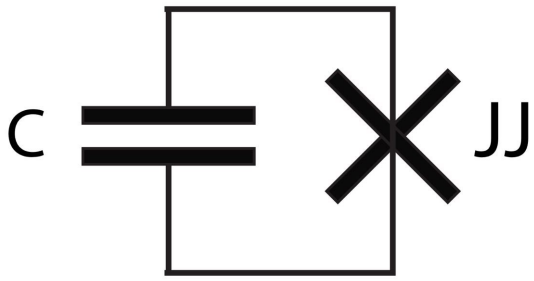

Figure 4: *Transmon circuit*

The hamiltonian of this circuit is :

$$H = \frac{Q^2}{2C} + E_J[1 - \cos(\delta)] \tag{17}$$

if we write the total charge of the capacitor as a function of the number of Cooper pairs we get:

$$\begin{aligned} H &= \frac{(2em)^2}{2C} + E_J[1 - \cos(\delta)] \\ &= 4E_C m^2 + E_J[1 - \cos(\delta)] \end{aligned} \tag{18}$$

Where m is the number of Cooper pair, and E_C is the charging energy. Similar to quantization of harmonic oscillator, here m and δ are canonical momentum and position for the transmon circuit. Therefore, we may transition to the quantum regime by promoting them to operators and then we arrive at the quantum hamiltonian.

$$H = 4E_C \hat{m}^2 + E_J[1 - \cos(\hat{\delta})] \tag{19}$$

To study the eigenvalues and eigenvectors of this Hamiltonian, let's put ourselves in the regime $E_J >> E_C$ i.e. $\delta << 1$. In fact we can expand in this regime the above hamltonian and we obtain the anharmonic oscillator :

$$H = 4E_C \hat{m}^2 + E_J \frac{\hat{\delta}^2}{2} - E_J \frac{\hat{\delta}^4}{24} \tag{20}$$

without getting lost in mathematics, we define in a similar way to the harmonic oscillator, operators of creation and destruction obtaining *[1]* [2] :

$$\begin{aligned} \hat{H} &= (\sqrt{8E_J E_C} - E_C)\hat{b}^\dagger \hat{b} - \frac{E_C}{2}\hat{b}^\dagger \hat{b}^\dagger \hat{b}\hat{b} \\ &= (\omega_J - E_C)\hat{b}^\dagger \hat{b} - \frac{E_C}{2}\hat{b}^\dagger \hat{b}^\dagger \hat{b}\hat{b} \\ &= \omega_{01}\hat{b}^\dagger \hat{b} + \frac{\alpha}{2}\hat{b}^\dagger \hat{b}^\dagger \hat{b}\hat{b} \end{aligned} \tag{21}$$

We get a hamiltonian for an anharmonic oscillator with an anharmonicity $\frac{\alpha}{2\pi}$ = - E_C and a lower energy transition ω_{01}.

[2] The mapping between this model and the LC circuit was done as follows $4E_C \rightarrow \frac{1}{2C}$, $\frac{E_J}{2} \rightarrow \frac{1}{2L}$ and $\omega_J = \sqrt{8E_J E_C} \rightarrow \omega_{LC} = \frac{1}{\sqrt{LC}}$

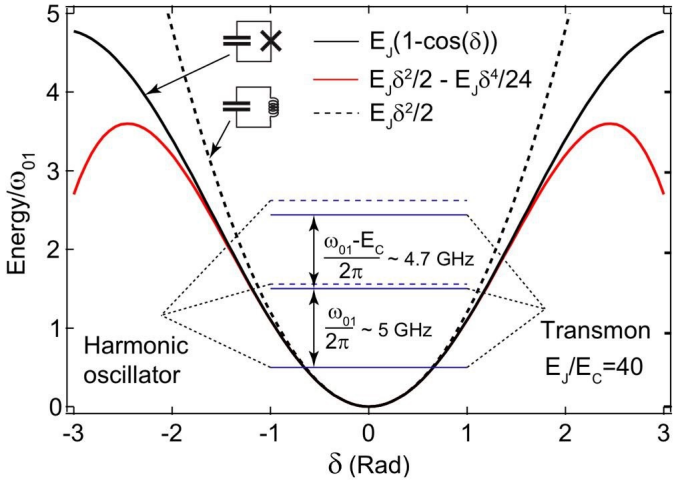

Figure 5: *energy levels with JJ versus harmonic oscillator energy levels* [1]

Therefore, under certain conditions of anharmonicity, we can consider our system as a two-level system described by the Hamiltonian:

$$\hat{H}_q = -\frac{\omega_q}{2}\hat{\sigma}_z \tag{22}$$

where $\omega_q = \omega_{01}$.

1.4 QUBIT-CAVITY INTERACTION

We now want to deal with the case of a qubit inserted in a cavity and study the total system.
Before starting, if we solve Maxwell's equations inside a cavity with given boundary conditions, we obtain a precise relationship that must satisfy the wave vector k. In general, we therefore say that the modes of the electro-magnetic field in a cavity are quantized.
We consider for our discussion only the lowest frequency mode of the field and that the qubit is placed in the center of the cavity. Given L the length of the cavity, supposing the characteristic dimensions of the qubit much smaller than L, we can assume that the qubit interacts only with the field at the point $\frac{L}{2}$ (we are imagining the field in a classical way).
The interaction between the qubit and the electric field is a dipole interaction which can be written with the following Hamiltonian :

$$\hat{H}_{interaction} = -\hat{d}\cdot\hat{E}_x(\frac{L}{2},t) \tag{23}$$

where $\hat{d}$ is the operator electric dipole of the qubit. Suppose the dipole is aligned with the field in the x direction, so $\hat{d} = d_x\sigma_x$, where d_x is the magnitude of the qubit dipole. We can write $\hat{d}$ as:

$$\hat{d} = d_x(\hat{\sigma}_+ + \hat{\sigma}_-) \tag{24}$$

Where $\hat{\sigma}_+$ ($\hat{\sigma}_-$) are the raising (lowering) operators for the qubit.
Recalling now that the electric field in second quantization is proportional to $\hat{E} \propto (\hat{a}^\dagger + \hat{a})$, we can rewrite the interaction hamiltonian like :

$$\hat{H}_{interaction} = -g(\hat{\sigma}_+ + \hat{\sigma}_-)(\hat{a}^\dagger + \hat{a}) \tag{25}$$

where g is equal to $d_x\mathscr{E}_0$ to quantify the interaction strength.
Now we have all the pieces to describe the combined qubit-cavity system.

$$\hat{H}_{tot} = \hat{H}_{qubit} + \hat{H}_{em} + \hat{H}_{interaction} \tag{26}$$

so,

$$\hat{H}_{tot} = \omega_c(\hat{a}^\dagger \hat{a} + \frac{1}{2}) - \frac{\omega_q}{2}\hat{\sigma}_z - g(\hat{\sigma}_+ + \hat{\sigma}_-)(\hat{a}^\dagger + \hat{a}) \tag{27}$$

We try to solve this Hamiltonian using the basis of the bare eigenfunctions.
We neglect the terms of the interaction that do not conserve the number of excitations, that is, we put ourselves in the limit in which it is permissible to do the rotating wave approximation (RWA). So we obtain :

$$\hat{H}_{tot} = \omega_c(\hat{a}^\dagger \hat{a} + \frac{1}{2}) - \frac{\omega_q}{2}\hat{\sigma}_z - g(\hat{a}^\dagger \hat{\sigma}_- + \hat{a}\hat{\sigma}_+) \tag{28}$$

This is called *Jaynes-Cummings* hamiltonian.
Even if this hamiltonian is described by a semi-infinite matrix, it is still possible to diagonalize it with the basis chosen exactly.

$$H_{JC} = \begin{pmatrix} \frac{1}{2}\omega_c - \frac{\omega_q}{2} & 0 & 0 & 0 & 0 & 0 \\ 0 & \frac{3}{2}\omega_c - \frac{\omega_q}{2} & g & 0 & 0 & 0 \\ 0 & g & \frac{3}{2}\omega_c + \frac{\omega_q}{2} & 0 & 0 & 0 \\ & & \cdots & & & \\ 0 & 0 & 0 & 0 & (n+\frac{1}{2})\omega_c - \frac{\omega_q}{2} & \sqrt{n+1}g \\ 0 & 0 & 0 & 0 & \sqrt{n+1}g & (n+\frac{1}{2})\omega_c + \frac{\omega_q}{2} \end{pmatrix} \tag{29}$$

We can see that the hamiltonian is block-diagonal and all the blocks follow a general form (except the first block which has only one element $\frac{1}{2}\omega_c - \frac{\omega_q}{2}$ corresponding to the absolute ground state of the system). So we only need to diagonalized individual blocks and the resulting eigenvalues of each block, indeed, are the eigenvalues of the entire hamiltonian.
Leaving aside mathematics, we obtain the eigenvalues from the diagonalization of the various blocks

$$\begin{aligned} E_g &= -\frac{\Delta}{2} \\ E_\pm &= (n+1)\omega_c \mp \frac{1}{2}\sqrt{4g^2(n+1)+\Delta^2} \end{aligned} \tag{30}$$

Where $\Delta = \omega_q - \omega_c$. The eigenstates associated with each of these eigenvalues are called the dressed states of the qubit and cavity

$$\begin{aligned} |0,-\rangle &= |g\rangle\,|0\rangle \\ |n,-\rangle &= \cos(\theta_n)\,|g\rangle\,|n+1\rangle - \sin(\theta_n)\,|e\rangle\,|n\rangle \\ |n,+\rangle &= \cos(\theta_n)\,|e\rangle\,|n\rangle + \sin(\theta_n)\,|g\rangle\,|n+1\rangle \end{aligned} \tag{31}$$

where $\theta_n = \frac{1}{2}\tan^{-1}(2g\sqrt{n+1}/\Delta)$. Basically these states are an overlap of where the excitement lies between the two systems.

1.5 DISPERSIVE APPROXIMATION

Now we focus only on the situation of dispersive regime that is $\Delta >> g$. We do this because it will help us to understand later how the measurements on the qubit are made, so this part is very important. In such situations, the interaction is relatively weak. Consider the unitary transformation

$$\hat{T} = e^{\lambda(\sigma_- a^\dagger - \sigma_+ a)} \tag{32}$$

where $\lambda = \frac{g}{\Delta}$. If we apply this transformation to the JC hamiltonian and we stop at the second order development since we are in the dispersive regime we get:

$$\hat{H}_{dis} = \omega_c \hat{a}^\dagger \hat{a} - \frac{1}{2}\omega_q \hat{\sigma}_z - \frac{g^2}{\Delta}\hat{a}^\dagger \hat{a}\hat{\sigma}_z \tag{33}$$

We can re-arrange the terms and we obtain

$$\hat{H}_{dis} = (\omega_c \mathbb{1} - \chi\hat{\sigma}_z)\hat{a}^\dagger \hat{a} - \frac{1}{2}\omega_q \hat{\sigma}_z \tag{34}$$

where $\chi = \frac{g^2}{\Delta}$.
So the beautiful result obtained is that depending on the state of our qubit the frequency of the cavity shifts by $\pm\chi$.

2 FABRICATION; *[5] [6] [1] [7]*

We start by choosing the materials. To reach higher coherence time we choose sapphire wafers because their loss tangent is less than silicon's.
The total energy decay rate such as a qubit can be understood as the sum of decay rates through all coupled loss channels. Equivalently, if the fraction of energy stored in each lossy element is known (the partecipation ratio p_i), then the qubit decay rate can be related to an intrinsic quality (or loss tangent $tan(\delta_i)$) of these elements:

$$\gamma = \sum_i \gamma_i + \Gamma = \omega \sum_i p_i \tan(\delta_i) + \Gamma \tag{35}$$

Here, i is the index indicating different spatial regions; p_i is the participation ratio (PR) of the i-th region, representing the proportion of the electric energy stored in that part to the total electric energy of the qubit; and tan $tan(\delta_i)$ characterizes the intrinsic dielectric loss of the i-th region and $\frac{\omega}{2\pi}$ is the qubit mode frequency and Γ accounts for ther types of loss mechanism, e.g. radiative decay. I also include the formula used to determine the participation ratio for completeness' sake.

$$p_i = \frac{\frac{1}{2}\epsilon_i \int_0^{t_i} dt \int_{S_i} |\vec{E}|^2 ds}{U_{tot}} \tag{36}$$

where t_i, ϵ_i, S_i and $\vec{E}$ are the thickness, dieletric constant, in-plane geometry, and electric field of the i-th interface region, and U_{tot} is the total electric energy of the qubit.
It's important to remember that sapphire functions well as a dielectric.
In this section, we'll look broadly at Josephson junction fabrication techniques. The following two cleanroom fabrication runs were performed to make electrical contact between the niobium pads and the junction in a 2D qubit without the usage of ion milling.
Then, using an impromptu sample, we investigated the effects of milling on various materials (niobium, aluminum, and sapphire).

2.1 JOSEPHSON JUNCTION FABRICATION

Aluminum on a sapphire wafer can be vaporized using an electron beam evaporator, which allows for directional evaporation, to create a Josephson junction.
The double angle evaporation method, which makes use of evaporation directionality, is what we use to fabricate JJ.
The spin coating of e-beam resist on a sapphire wafer, the deposition of a thin aluminum layer, e-beam lithography, development, pre cleaning, double angle evaporation, lift off, and post cleaning are typical steps in the JJ fabrication process.
E- beam resist: we use a stack of two resists for junction fabrication. The bottom layer (MMA) is more sensitive than the top layer (PMMA) to e-beam exposure.
The reason for this choice of resist staking is to achieve a wide undercut which is convenient for clean lift-off as depicted in *Figure 6a-6b*.
It also enables for a suspended bridge needed for junction fabrication (*Figure 6c)*.
The resist layers can be coated on the substrate by spin-coating. The thickness of the layers is controlled by the spinning velocity, the total time of spinning, and the viscosity of the resist. In particular we spin coat MAA(8.5)MAA copolymer EL11 at 4000 rpm (to get ~ 500 nm of thickness) and than we spin coat 950K PMMA a A4 at 4000 rpm (to get ~ 200 nm of thickness).

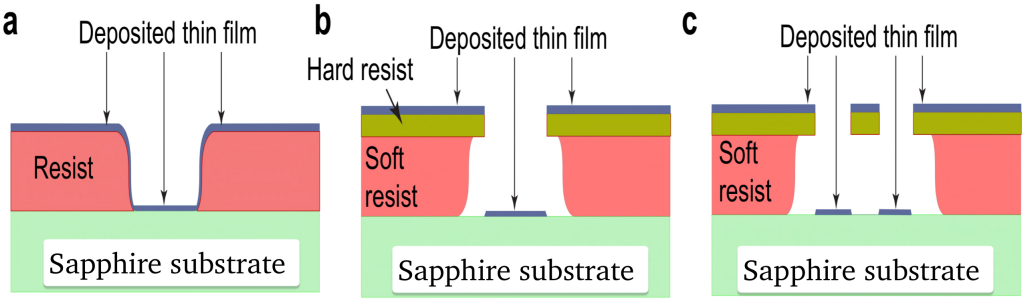

Figure 6: ***a*** *With a single layer of resist, it is often difficult to get small and clean patterns. Mainly because the wall of the resist may also get deposited which connects top layers to the bottom layers which make it difficult to properly lift-off the resist without peeling off the actual pattern.* ***b*** *This issue can be avoided by using two layers of the resist. The top layer provides sharp edges as a mask and the bottom layer act as a spacer. The proper amount of undercut aids the liftoff process.* ***c*** *Moreover, the undercut of the lower resist can be used to created suspended resist (free-standing bridge) which is used for the JJ fabrication in double angle evaporation.*

- **Deposition of thin aluminum layer**: As a result of the sapphire wafer we employ, we are required to deposit a thin layer of aluminum for discharge; otherwise, there is a chance that the charge on the sapphire would affect the electron beam during lithography. This thin aluminum layer is deposited for evaporation. In our experiments we deposit 25 nm.

- **Electron-beam lithography**: we use a focused beam of electrons for patterning the polymers.

- **Resist development and pre-cleaning**: we develop the polymers. In particular we use AZ MIF 300 developer to remove the aluminum layer and than MIBK:IPA(1:3) to remove the exposed resists.

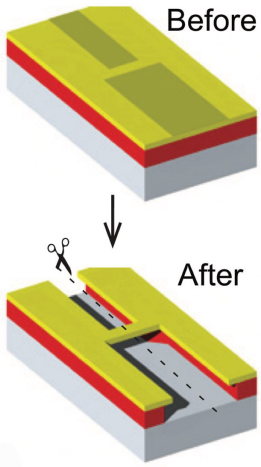

Figure 7: *Before and after the development*

- **Electron-beam evaporation**: We use a double angle evaporation method to fabricate JJs as depicted in *figure 8* [3]. We use aluminum for the JJs because we know the growth of aluminum oxide.
  First we deposit aluminum, than we wait for aluminum oxide growth (we create the insulator barrier) the last passage is the second evaporation.

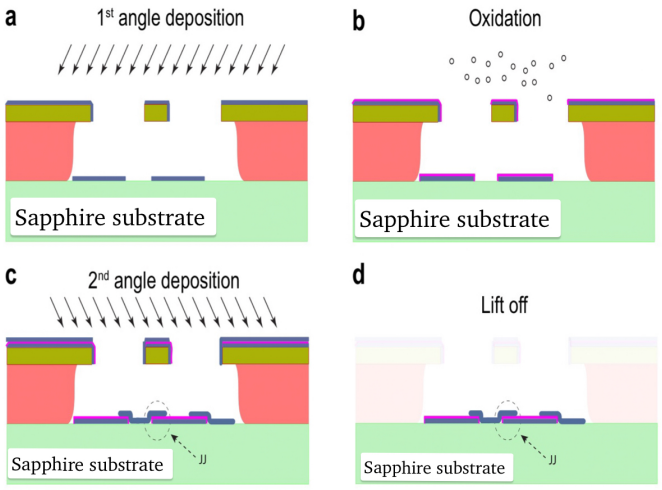

Figure 8: *steps of double angle evaporation technique*

- **Lift-off**: we use acetone to dissolve the resist which leaves behind the JJ on the substrate.

We now need to specify how the electrical contact between the Niobium pads and Josephson Junction could be made. Up to now they have used ion milling to the Niobium pads on sapphire substrate to remove Niobium oxides . But in order to increase the coherence time, we have used a method called "patching." (Lithography masks are used to produce niobium pads.)

2.2 ELECTRIC CONTACT WITH ION MILLING

Before the deposition of the Josephson Junctions on Niobium pads we do ion milling to remove the oxides. We do ion milling with three different angles using the same apparatus that we will use for ShET later. We use this technique to hollow out the sapphire wafer as homogeneously as possible. We do this because we are unable to do ion milling on niobium alone. So, this technique creates an irregular substrate for the junction.

2.3 PATCHING

We place the JJ on the Niobium pads using this alternative method. We completed two alternative forms of this deposition; the reason behind our decision is discussed in the section below. The JJs were placed on the Niobium pads the first time, then to shield the junctions from any charge accumulation, JJs are placed between the pads.
Unfortunately, in the first situation there is no electrical contact between JJs and pads due to the buildup of oxides, and in the second scenario there is no electric contact due to the absence of a contact in addition to the oxides. We employ a method called "*patching*" to make the electrical contact.
To create the electric contact we use, like for the junction, a stack of two resists and on the top a thin aluminum layer (for discharge) . In this instance, a tiny layer of aluminum is deposited for evaporation so that

[3] we use +22ř and −22ř as angles.

no electrons are present to potentially harm the junction.
To print the bandages on the transmon, we are currently using electron beam lithography. After removing the aluminum, we will develop the resists.
To get rid of the niobium and aluminum oxides, we now use ion milling. Finally, aluminum is deposited to make the electrical connection between the pads and JJs. "Patching" is the name of this procedure. Also when we deposit JJs between the pads we use the patching, the only difference is that the electric contact is established between the parts only at the end.

3 RESISTANCE MEASUREMENTS

It is crucial to measure the resistance of junctions at room temperature since this resistance and the junction's critical current are correlated, and by fixing the critical current we can fix the qubit frequency.

$$I_c = \frac{\pi\Delta(0)}{2eR_n} \tag{37}$$

With $\Delta(0)$ is the gap of superconductor at T = 0 K, for aluminum $\Delta(0) \sim 170\mu eV$, R_n is the normal resistance of the junction at room temperature. So, for a certain qubit design, E_c is fixed and the qubit frequency is

$$\omega_q = \sqrt{8E_jE_c} - E_c \tag{38}$$

where E_j is the Josephson energy

$$E_J = \frac{\hbar}{2e} I_c \tag{39}$$

3.1 RESISTANCE MEASUREMENTS, JJS ON THE PAD

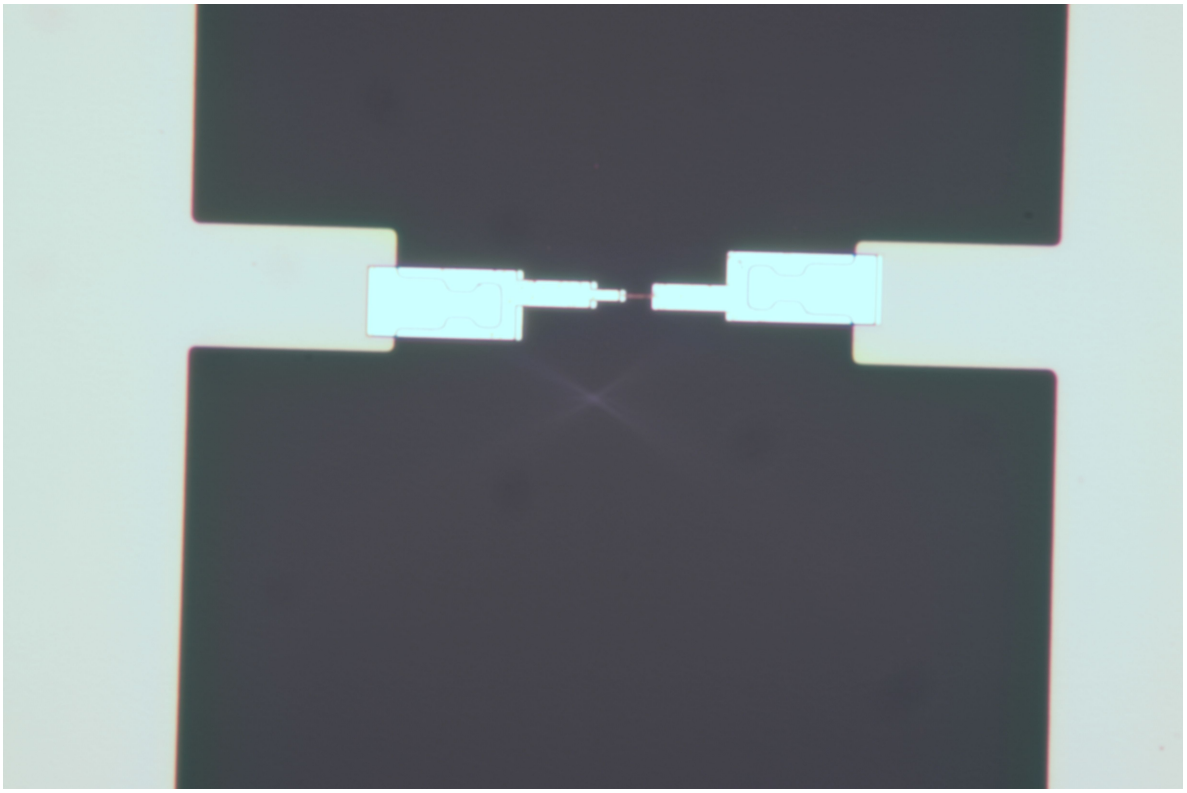

Figure 9: *Optical microscope image of a Josephson junction. Case of overlay between JJ and pads*

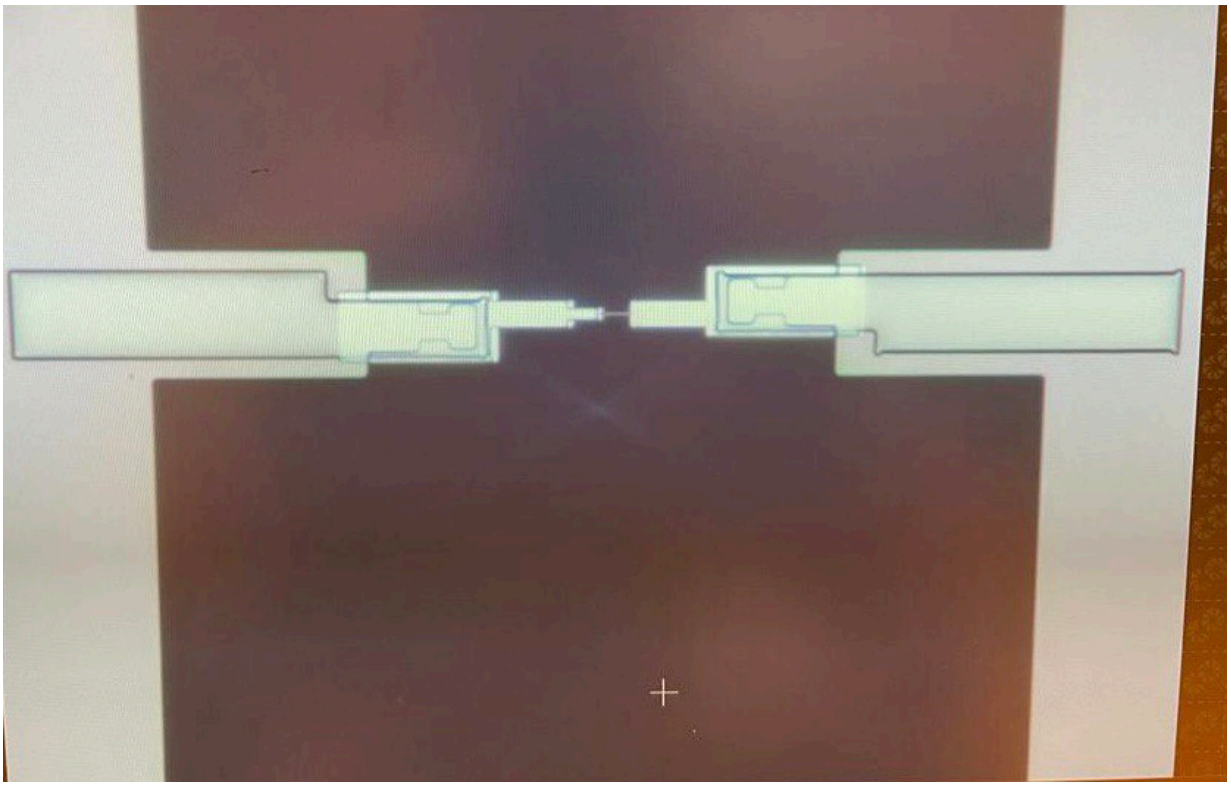

Figure 10: *Optical microscope image of Josephson junction with patching*

We measured resistance once our JJ were ready. In our experiments, we constructed 100 Josephson junction of various sizes. Particularly, only having resistances of around 10 K Ω are of interest to us.

RESISTANCE [KΩ] JJs ON THE PADS										
JJ [μm^2]										
0.014	600	600	600	600	600	600	600	600	600	600
0.018	600	600	600	600	600	600	600	600	600	600
0.023	600	600	600	600	600	600	600	600	600	600
0.030	600	600	10.4	600	600	600	600	600	600	600
0.039	9.35	600	600	600	600	600	600	600	600	600
0.050	600	8.34	7.64	600	8.43	600	8.41	8.51	600	600
0.061	6.50	600	600	7.20	7.35	6.14	7.17	600	600	600
0.072	5.85	6.16	5.89	600	6.03	5.97	600	7.43	6.27	600
0.090	600	4.79	4.92	4.85	600	4.76	5.08	4.81	5.08	5.01

Table 1: *Resistance measurements of JJs on the pads*

These measurements show that nearly all connections with minor dimensions are non-functional. At first, we believed that the fallen bridge was to blame for the lack of current flow in the junction (in fact 600 KΩ is the resistance in parallel to the junction of our instrument).
But later, when we examined these junctions under an optical microscope, we discovered that there was actually no current flow because the aluminum of the junction melted, creating an ESD damaged junction.

Figure 11: *Damaged junction possibly due to ESD event*

The minuscule junctions may not have been adequately protected from outside charges by the thin aluminum layer intended for discharge, which is why a buildup of charge may have broken the junction. Because they are more robust, the larger junctions are still alive.
A fairly straightforward equipment is used to measure these resistances. We have two tips, and we set the instrument's resistance to 5 Ω while applying the tips to the sample. Therefore, there is no current through the junction if one tip is applied to the Noibium pads before the other. We change the instrument's resistance to 600 K Ω after applying the tips. As a result, we measure the junction's resistance. The instrument's extremely basic design is seen below.

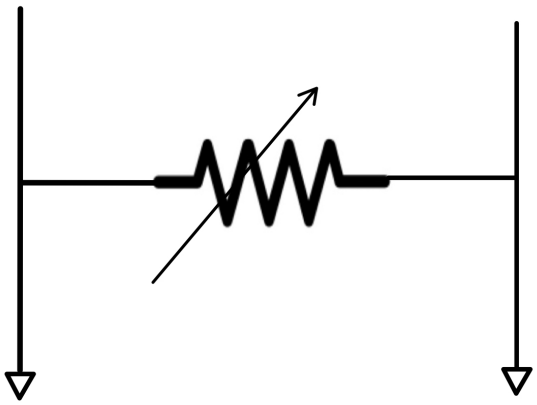

Figure 12: *Design of instruments. We can change this resistance between 5 Ω and 600 k Ω.*

3.2 RESISTANCE MEASUREMENTS, JJS BETWEEN THE PAD

First of all, as depicted in the picture below, we can see the differences from the previous experiment. The Josephson junction doesn't touch the pads.

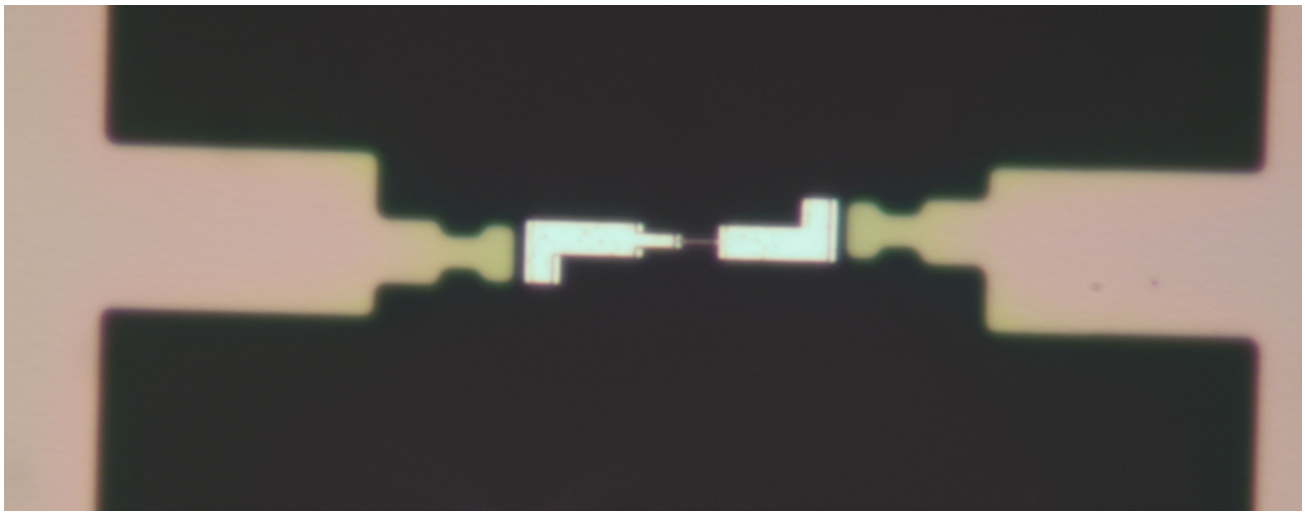

Figure 13: *No overlay*

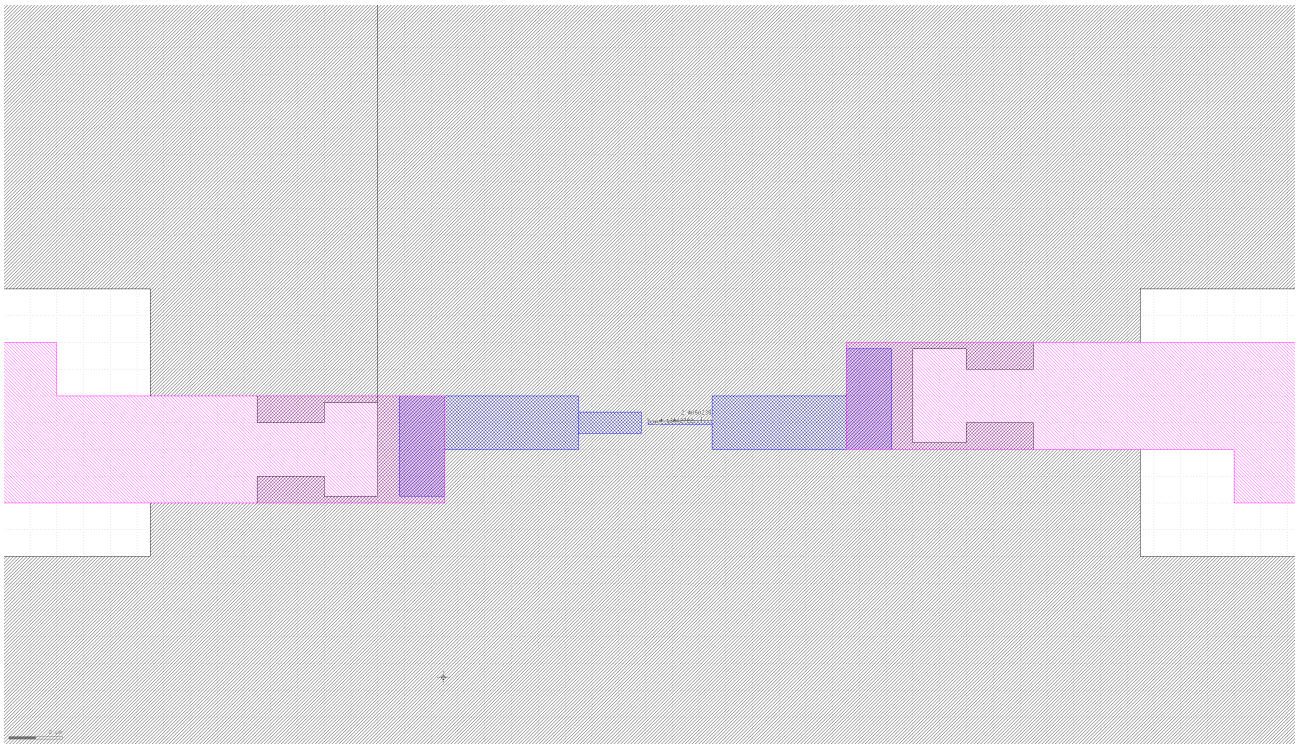

Figure 14: *No overlay with patching, screenshot file gds.In order to simplify my interpretation of the image, I have decided to delete the undercut.*

To give greater protection from possible accumulations of charge at the junction, we decided in this second experiment to deposit them between the two pads so as to have electrical contact only at the end with the bandaids.
In fact, as we can see from the table below, with this technique many more junctions are functional, especially among those of small dimensions.

RESISTANCE [KΩ] JJs BETWEEN THE PADS					
JJ [μm^2]					
0.014	39.7	20.2	20.3	300	19.1
0.018	600	16.3	150	400	17.7
0.023	220	600	0.12	47	16.0
0.030	22	13.1	11.8	1.4	13.1
0.039	600	40	10.9	70	0.170
0.050	9.3	600	0.126	11.0	10.0
0.061	8.9	8.8	0.160	9.3	9.4
0.072	7.70	8.0	7.2	500	7.40
0.090	500	13.5	600	6.78	6.26

Table 2: *Resistance measurements of JJs between the pads*

I used Python to perform a linear fit after these results to establish a direct correlation between normal resistance and Josephson junction surface.
Once we have a fixed capacitor size, we can therefore use this plot to generate the transmon qubit at the appropriate frequency.

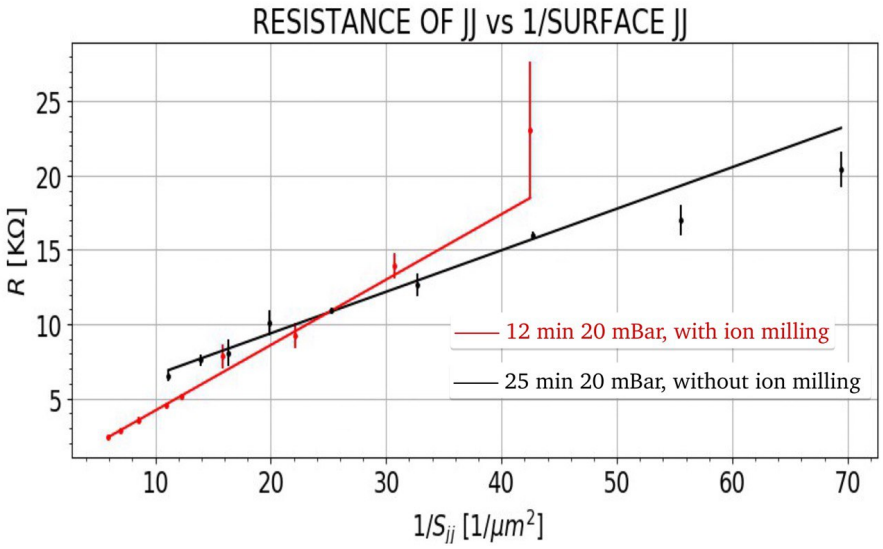

Figure 15: *Two linear fits of two different arrays of Josephson junction. One constructed using ion milling, the other not.*

3.3 MILLING TEST

The goal of this experiment is to find the shortest possible period that will allow the oxide on the Niobium pads to be removed. As a result, we minimize sapphire etching.
Using the methods described above, we produced a specific sample. This sample's surface was made of three different materials: sapphire, aluminum, and niobium. At this point, we have used ion milling for various lengths of time, and after that, we have examined how much the various materials have been etched. We have done two experiments, one with 30 sec, for each angle, of ion milling and the other with 45 sec always for each angle. After that, we used MikTek's profilometer to measure the etching.

4 QUBIT CHARACTERIZATION; *[1]*

We examine the cavity-qubit system within the refrigerator in this part. The minimum circuitry inside the fridge is depicted in figure 16.

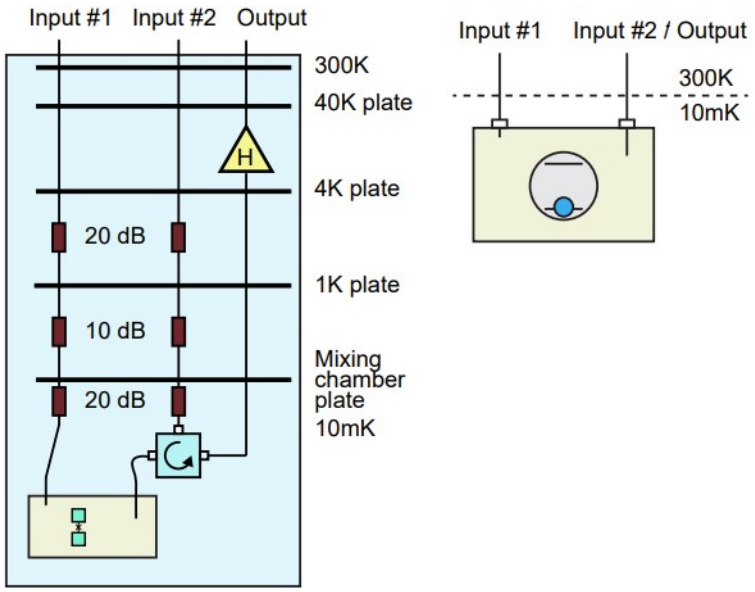

Figure 16: *The minimum experimental setup for basic qubit characterization*

The main qubit characterization includes five basic experiments:

- "punch out"
- Two-tone spectroscopy
- Rabi measurements
- T_1 measurements
- Ramsey measurements

The first two experiments are in the frequency domain which means we only look at scattering parameters of the system for characterization. However, the last three experiments are measured in the time domain and involve preparation and readout of the qubit state. We examine only the first two.

4.1 "PUNCH OUT"

The qubit must first be determined to be "alive" or not. For so, we must determine whether the cavity frequency changes in response to the qubit's state. As we have seen at the theoretical level in 1.5.
Simply compare the cavity's transmission (or reflection) at low power to high power to see whether the cavity's frequency varies. We can be fairly certain that a qubit is in its ground state when we use extremely modest power to probe the cavity. Therefore we measure the resonance frequency of cavity when qubit is in the ground state. Next, we turn up the power of the VNA to a very high power. In this case, we send a huge amount of photons into the cavity which essentially overwhelms the qubit. Basically, the driving amplitude is so high that the induced current exceeds the critical current of the junction. Practically, in such a high power regime, we measure the bare cavity frequency. Now if there is a working qubit inside the cavity we can see the cavity frequency shift and we say that the cavity "punched out".

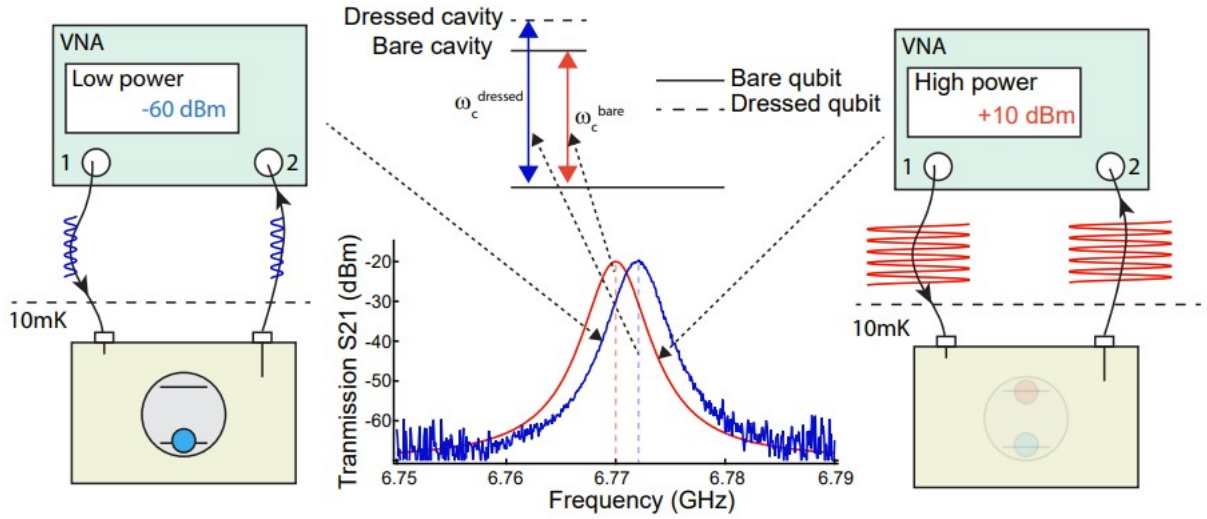

Figure 17: *The "punch-out" measurement*

4.2 TWO-TONE SPECTROSCOPY

Knowing that the qubit is working, the next step is to find the qubit frequency. The idea is to continuously send a weak microwave signal to the cavity at the low power cavity resonance (the cavity frequency when the qubit is in the ground state) and probe the cavity transmission.
Therefore, we constantly receive a high transmission signal because we probe at the resonance of the cavity. While this first tone is on, we start sending another microwave signal (labeled as BNC [4]) into the cavity.
We sweep the frequency of the probe tone BNC and monitor the cavity transmission. During the sweep, once the BNC frequency hits the qubit transition frequency (BNC= ω_q), it excites the qubit therefore the state of the qubit is no longer in the ground state (on average) and that causes a shift in the cavity frequency. Now, because the VNA frequency (which is fixed) is no longer resonant with the cavity, the transmitted power drops. If we increase the BNC signal amplitude (by $\sim$ 10 dBm), we can also see a second dip at a slightly lower frequency. This dip corresponds to the process by which two photons excite the qubit from the ground state to second excited state, $|g\rangle \rightarrow |f\rangle$. The second dip gives a useful piece of information which allows us to simply calculate the transmon anharmonicity.

[4] BNC is the name of generator

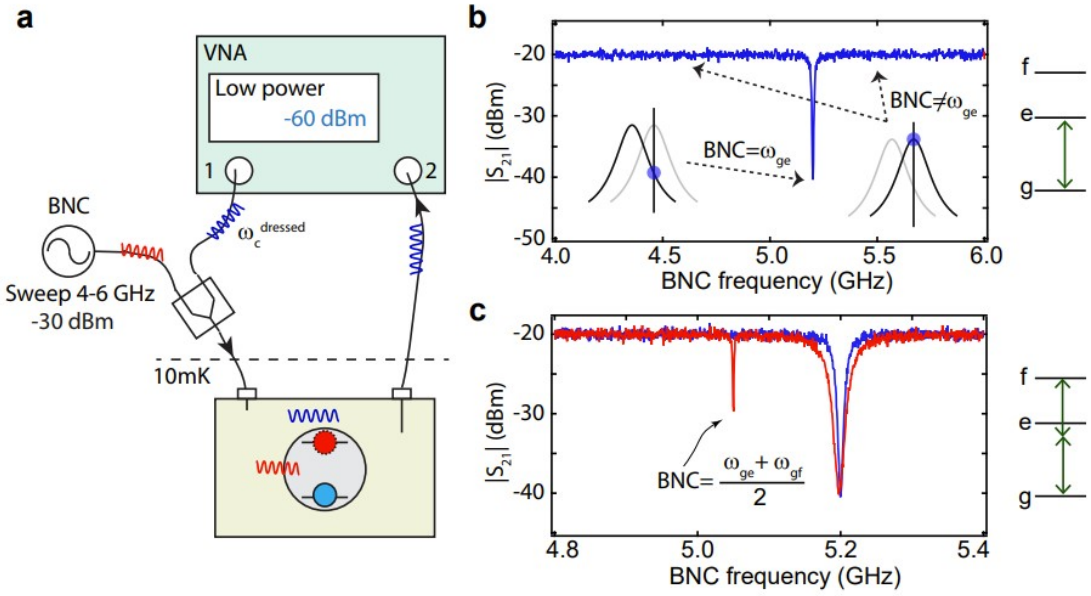

Figure 18: *Two-tone spectroscopy*

APPENDIX A **CAVITY RESONATORS;** *[8]*

We want to see the electric field between the plates of a circular capacitor at high frequency. If we apply a constant pd (potential difference) across the capacitor then the field in the capacitor will be static.
The situation changes if we connect it to an alternating voltage generator. When the voltage reverses, the positive charge of the top plate is taken away and is replaced by a negative charge; as this happens, the electric field disappears and then reforms in the opposite direction. As the charge slowly swings back and forth, the electric field follows.
Neglecting the effect at the edges we can write:

$$E = E_0 e^{i\omega t} \tag{40}$$

with E_0 is a constant.
As the electric field changes inside the capacitor, the flux within the circuit changes ,thus generating a magnetic field

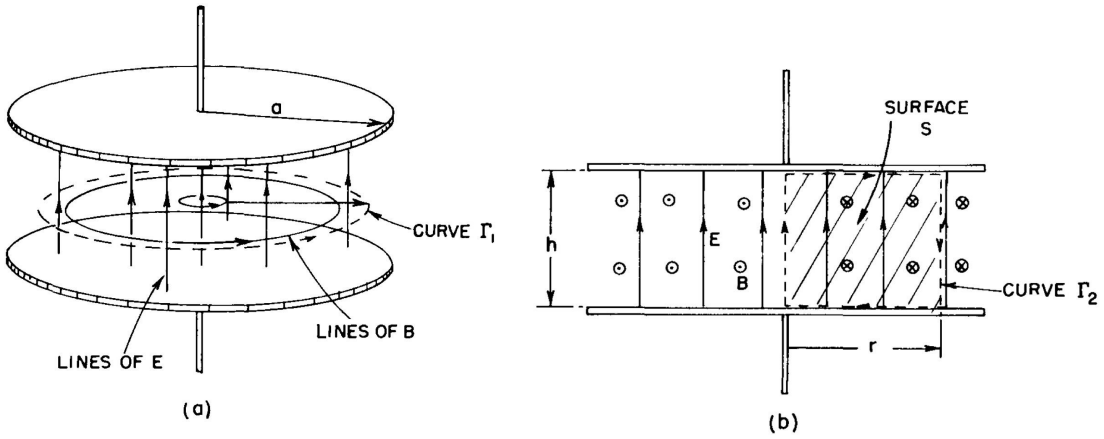

Figure 19: *The electric and magnetic field between the plates of a capacitor*

Let's try to calculate this magnetic field with Maxwell's equations:

$$c^2 \oint_\Gamma \vec{B} \cdot d\vec{s} = \frac{\partial}{\partial t} \int_{inside\,\Gamma} \vec{E} \cdot \vec{n} da \tag{41}$$

so we obtain :

$$B = \frac{i\omega r}{2c^2} E_0 e^{i\omega t} \tag{42}$$

If the frequency increases the magnetic field increases accordingly. However, if we have a magnetic field that varies, the electric field in the capacitor cannot absolutely be uniform by the law of Faraday.
So we can calculate the correction to the electric field found first with faraday's law.

$$E = E_1 + E_2 \tag{43}$$

E_1 is the uniform field found earlier and $E_2$is the correction.

$$\oint_{\Gamma_2} \vec{E} \cdot d\vec{s} = -\frac{\partial}{\partial t} \int_{inside\,\Gamma_2} \vec{B} \cdot \vec{n} da \tag{44}$$

E_1 is zero in this integral only E_2 contributes, and its integral is just $-E_2 h$, where h is the spacing between the plates. While B changes only with r and not with h so :

$$E_2(r) = \frac{\partial}{\partial t}\int B(r)dr$$
$$E_2(r) = -\frac{\omega^2 r^2}{4c^2}E_0 e^{i\omega t} \tag{45}$$

Similarly, we can continue to find fixes for fixes. Doing all the math we finally get the following series for the electric field[5]:

$$E = E_0 e^{i\omega t}[1 - \frac{1}{(1!)^2}(\frac{\omega r}{2c})^2 + \frac{1}{(2!)^2}(\frac{\omega r}{2c})^4 - \frac{1}{(3!)^2}(\frac{\omega r}{2c})^6 + ...] \tag{46}$$

if we define

$$J_0(x) = 1 - \frac{1}{(1!)^2}(\frac{x}{2})^2 + \frac{1}{(2!)^2}(\frac{x}{2})^4 - \frac{1}{(3!)^2}(\frac{x}{2})^6 + ... \tag{47}$$

so we can write

$$E = E_0 e^{i\omega t} J_0(\frac{\omega r}{c}) \tag{48}$$

$$B = \frac{i\omega r}{2c^2}E_0 e^{i\omega t} J_0(\frac{\omega r}{c}) \tag{49}$$

Let's see whether J_0 does go trough zero and become negative. If we make the calculation more accurate we find that it goes trough zero at x = 2.405. Below there is the graphic of the function

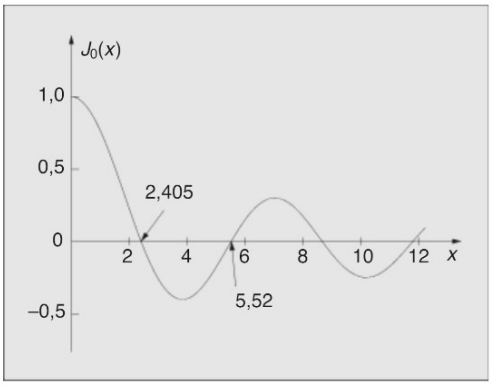

Figure 20: *The Bessel function* $J_0(x)$

So we can see that for high frequency at the center of the cavity the field is opposite to the outermost one, therefore this object is very complex to treat for high frequencies.
Now given our parallel flat plate capacitor of fixed radius r, we set the frequency such that the relation is satisfied

$$\omega = \frac{2.405c}{r} \tag{50}$$

So if we now close our capacitor with a very thin conductive foil, this since it is inserted where the fields are zero does not involve any modification to the system.
And then given the initial impulse at the correct frequency, if we subsequently detach the wires from the generator we have created a region of space in which the field is self-powered, a resonant cavity.
On parallel flat plates, however, due to the large divergence of the electric field there will be a strong accumulation of charge. However, since the electric field is vertically oscillating this charge will have to reverse

[5] we set the field in the center of the capacitor equal to $E = E_0 e^{i\omega t}$, so that in the center there are no corrections

itself from one face to the other, creating surface currents that generate dissipation in our cavity.
If now we make two small side holes on the walls of the jar and insert two coils, one in which we circulate alternating current to operate the fields and one attached to a current detector and we measured the intensity of current as a function of the frequency of the generator we would see

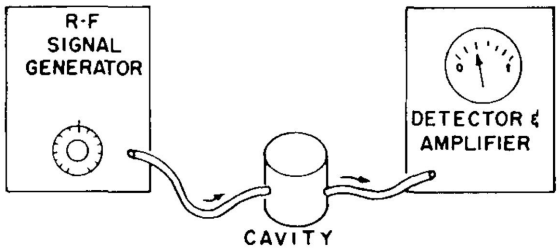

Figure 21: *A setup for observing the cavity resonance*

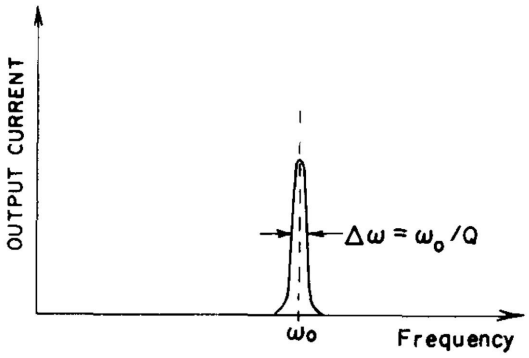

Figure 22: *The frequency response curve of a resonant cavity*

Where Q is the quality factor of the cavity.

REFERENCES

[1] Mahdi Naghiloo. “Introduction to experimental quantum measurement with superconducting qubits . (English)”. In: *arXiv* (2019).

[2] Jens Koch et al. “Charge insensitive qubit design derived from the Cooper pair box . (English)”. In: *arXiv* (2007).

[3] A.C. Rose-Innes and E.H. Rhoderick. *Introduction to superconductivity*. Pergamon, 1978. ISBN: 9780080216515.

[4] R. Loudon. *The quantum theory of light*. Oxford University press, 2000.

[5] Alexander Bilmes et al. “In-situ bandaged Josephson junctions for superconducting quantum processor ”. In: *IOPscience- Superconductor Science and Technology* 34.12 (2021).

[6] Ani Nersisyan. “Manufacturing low dissipation superconducting quantum processors . (English)”. In: *arXiv* (2019).

[7] J. Verjauw et al. “Investigation of Microwave Loss Induced by Oxide Regrowth in High-Q Niobium Resonators . (English)”. In: *Phys. Rev. Applied* (2021).

[8] Richard P. Feynman, Robert B. Leighton, and Matthew Sands et al. *The Feynman Lectures on Physics; Vol. I*. American Association of Physics Teachers, 1965.